J Fluoresc (2015) 25:69–78
DOI 10.1007/s10895-014-1481-1

ORIGINAL PAPER

NIR-Emitting Boradiazaindacene Fluorophores -TD-DFT Studies on Electronic Structure and Photophysical Properties

Kishor G. Thorat · Hanusha Bhakhoa · Ponnadurai Ramasami · Nagaiyan Sekar

Received: 25 September 2014 / Accepted: 24 November 2014 / Published online: 11 December 2014

Abstract Density Functional Theory [B3LYP/6-31G(d)] and Time Dependent Density Functional Theory [TD-B3LYP/6-31G(d)] computations have been used to have more understanding of the structural, molecular, electronic and photophysical parameters of recently synthesized near IR-emitting acid switchable di-styryl BODIPY dyes. The structures have been optimized using function B3LYP and basis set used was 6-31G(d) for all the atoms and their geometries which are correlated with corresponding rotational isomers including rotational isomers of diprotonated forms in chloroform solvent. The observed energies of the optimized molecules suggest that there may be rotation about C-C single bond as the observed energy barrier is very low. The results of TD-DFT suggest that there is very good match between the observed and calculated absorptions diprotonated forms of one molecule. There is also good match between experimental and theoretical emission of neutral forms. More deviations are observed in the case emission of the diprotonated forms.

Electronic supplementary material The online version of this article (doi:10.1007/s10895-014-1481-1) contains supplementary material, which is available to authorized users.

K. G. Thorat
Tinctorial Chemistry Group, Department of Dyestuff Technology, Institute of Chemical Technology, N. P. Marg, Matunga, Mumbai 400 019, Maharashtra, India

H. Bhakhoa · P. Ramasami (✉) · N. Sekar (✉)
Computational Chemistry Group, Faculty of Science, Department of Chemistry, University of Mauritius, Réduit, Mauritius
e-mail: ramchemi@intnet.mu
e-mail: n.sekar@ictmumbai.edu.in

N. Sekar
e-mail: nethi.sekar@gmail.com

P. Ramasami
Department of Pharmaceutical Chemistry College of Pharmacy, King Saud University, P.O. Box. 2457, Riyadh 11451, Kingdom of Saudi Arabia

Keywords NIR-BODIPYs · Boradiazaindacenes · DFT · TD-DFT · Dipole moment · Fluorescent di-styryl BODIPYs

Introduction

Difluoroboraindacene (BODIPY) dyes discovered about 45 years ago [1] have become interesting class of highly fluorescent dyes and are used in several fields, as fluorescent labels [2], chemosensors [3–10], dye-sensitized solar cells [11, 12], and for photodynamic therapy [13]. Very good photophysical properties such as high fluorescence quantum yields (typically ranging from 0.6 to 1.0), high molar extinction coefficients, good photostability and sharp absorption-emission bands in the visible region of spectrum are the reasons for their use in bioimaging, lasers applications, bio-labels and cation sensing [13–15]. But typical BODIPY molecules absorb near 510–520 nm and emit at around 540 nm, considerably shorter wavelength region than what is referred to as the "optical window" (650–900 nm) that is required for a fluorophore to be useful for biological applications. The fluorophores showing photophysics in the region, 650–900 nm, are very useful as there would be significant reduction of background signal due to auto-absorption and auto-fluorescence of biomolecules in this region of electromagnetic spectrum. In addition, there will be deep penetration of near IR light, little cell rupture and low light scattering with the possibility to use low cost excitation light source [16].

The photophysical properties of a typical BODIPY dye can easily be tuned by modifications at various positions of boradiazaindacene core, like introduction of electron donating moieties at 3 and 5 positions [17, 18], replacement of *meso* C atom by N atom [19, 20], making rotatable moieties rigid [21–23], extension of conjugation by fusion of aryl moieties [24–28], and extension of π conjugation by the introduction styryl subunits at 3- and 5-positions of the BODIPY core [29, 30].

A similar approach of extending π conjugations by the introduction styryl subunits at 3- and 5- positions of BODIPY core in order to get BODIPY fluorophore emitting near IR has been used many times by numerous groups [31]. The fact that the presence of suitable substituents determines the utility of a fluorophore in the near IR region of the electromagnetic spectrum like metal ion sensors when the substituent bears binding site for metal ions [32, 33], molecular imaging and cell labelling [34], molecular switches [29], fluorescent DNA intercalating probes [35], one- and two-photon fluorescence imaging of living cells [36], as molecular switch [37], in dye-sensitized solar cells [38–40], energy transfer cassettes [41–43] and pH sensors [29, 44, 45].

In 2008 Deniz E; *et al.* [31] reported the synthesis and photophysics of two interesting NIR emitting 3, 5-distyryl substituted BODIPY fluorophores, **1 EE** and **2 EE** (Fig. 1), and proved that these NIR-emitting fluorophores can be used as ratiometric probes for pH. Moreover, the two molecules were designed in such a way that upon protonation using trifluoroacetic acid in chloroform one shows a red shift while the other shows a blue shift [31]. The near IR-emitting di-styryl substituted BODIPY, **2 EE**, has also been studied by authors with single-crystal X-ray crystallography and suggested that the two styryl subunits are oriented in *trans* fashion. To this end we have made an attempt to investigate optimised geometries of the molecules, **1 EE**, **2 EE** and their corresponding mono- and di-protonated forms. Also we have made an attempt if there is any possibility of rotation of styryl subunit/s along C_1-C_{23}/C_{55}-C_{78} single bond/s and related their optimised geometries, energies, dipole moments, vertical excitation and emissions with **1 EE**, **2 EE** and their corresponding mono- and di-protonated forms using DFT and TD-DFT computations using B3LYP/6-31G(d) level of theory.

Materials and Methods

Computation Strategy

All the computations were performed using the Gaussian 09 program package [46]. The ground state (S0) geometry of the dyes was optimized using DFT [47] method. The functional used was B3LYP, (the B3LYP combines Becke's three parameter exchange functional (B3) [48] with the nonlocal correlation functional by Lee, Yang and Parr (LYP) [49]). The basis set used in both, DFT and TD-DFT methods for all the atoms was 6-31G(d). In order to verify whether the optimised structures have minimum energy, frequency computations were performed at the same level of theory. The vertical excitation energies and oscillator strengths were obtained for the 20 lowest S0-S1 transitions at the optimized ground state equilibrium geometries by using the Time Dependent Density Functional Theory (TD-DFT) using the same hybrid functional and basis set [50–56]. To obtain their minimum energy geometries (which correspond to the emissive state) the low-lying first singlet excited states (S1) of the dyes were relaxed using the TD-DFT. The energy difference between the optimized geometries at the first singlet excited state and the ground state was used in calculating the emission [57]. The frequency computations were also carried out at the same level of theory on the optimised geometry of the first excited state of the dyes. All the computations in the chloroform media were carried out using the Self-Consistent Reaction Field (SCRF) under the Polarizable Continuum Model (PCM) [58, 59]. The electronic absorption spectra, including wavelengths, oscillators strengths, and main configuration assignment, were systematically investigated using TD-DFT with PCM model on the basis of the optimized ground structures, emissions were calculated using TD-DFT from optimised structures in the excited state at B3LYP/6-31G(d) level of theory.

Here we also considered a) corresponding di protonated forms **1-2H EE** and **2-2H EE** respectively and tried to investigate and correlate their properties with experimental one and that of corresponding neutral molecules **1 EE** and **2 EE**, and b) studied the properties of the possible rotamers, **1 EZ** and **2 EZ**, obtained after the rotation of C-C single bond of one of the styryl subunit and correlate their structural and photophysical properties with that of corresponding parent molecules, **1 EE** and **2 EE** respectively (Fig. 1).

Results and Discussion

Geometrical Parameters

The structures of reported dyes [31], **1 EE** and **2 EE**, their diprotonated forms and corresponding possible rotamers are shown in Fig. 1. The ground state geometries of the dyes **1 EE**, **1 EZ**, **2 EE**, **2 EZ** and their corresponding diprotonated forms, **1-2H EE**, **1-2H EZ**, **2-2H EE**, **2-2H EZ** respectively are optimized by DFT and the results of this study are presented in Tables 1 and 2. The C_9BF_2 framework of **1 EE**, **1 EZ**, **2 EE**, **2 EZ** and their corresponding diprotonated forms **1-2H EE**, **1-2H EZ**, **2-2H EE**, **2-2H EZ** are almost planer with boron atom displaced from the median plane by only 4.2 to 5.5°. The styryl subunits are having almost coplanar arrangement with the BODIPY (C_9BF_2) core with a little twist of 4.2 to 5.5° and 4-methyl phenyl substituent at *meso* position show orthogonal arrangement with the dihedral angles 89.8°, 89.8°, 84.5°, 79.8° in dyes **1 EE, 1 EZ, 2 EE** and **2 EZ**, 85.4°, 89.9°, 83.1.5°, 81.1° in dyes **1-2H EE, 1-2H EZ, 2-2H EE** and **2-2H EZ** respectively and is electronically decoupled from the BODIPY core.

The resulting ground state optimized geometry of dye **1 EE** and **1-2H EE** is such that it has small dihedral angle C_{56}-C_1-C_{23}-C_{25} with one of the styryl subunit is off the C_9BF_2 plane as 5.44 and 5.48° and the other styryl subunit making dihedral

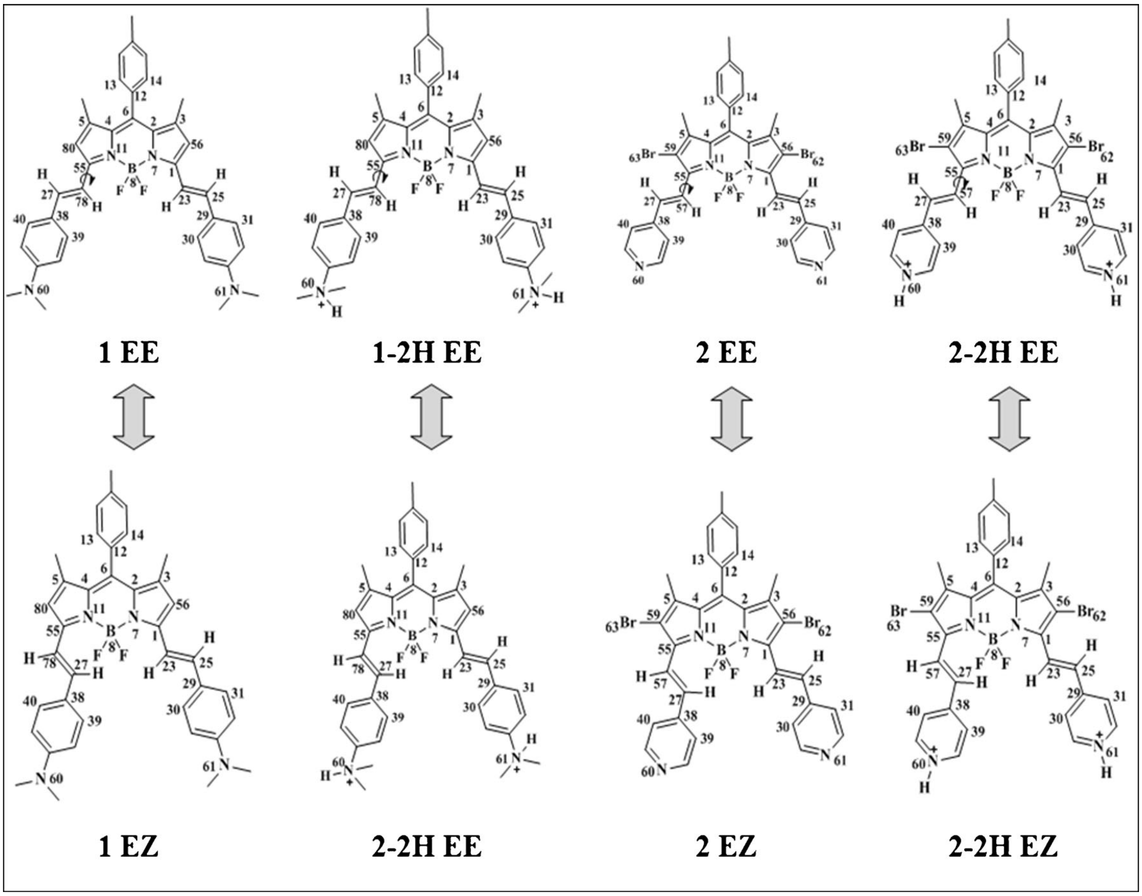

Fig. 1 Possible structures of di-styryl BODOPY molecules, 1 EE and 2 EE, before and after Di-protonation and rotation about C-C single bond of one of the styryl subunits

angle C_{80}-C_{55}-C_{78}-C_{27} with C_9BF_2 plane as 5.43 and 4.82° respectively (Table 1).

The excited state optimized geometry reveals that the styryl subunits become more planar in dye **1 EE** with a decrease in dihedral angle (C_{56}-C_1-C_{23}-C_{25} and C_{80}-C_{55}-C_{78}-C_{27}) by 1.02 and 1.01° respectively. Contrary to this is the observation with the corresponding di-protonated form, **1-2H EE**, in which there is an increase in dihedral angles (C_{56}-C_1-C_{23}-C_{25} and C_{80}-C_{55}-C_{78}-C_{27}) making the two styryl subunits displaced more from C_9BF_2 median plane by 0.96 and 0.84° respectively in excited state.

Upon protonation of the molecule **1 EE** to **1-2H EE**, the ground state optimized geometry reveals that a major bond lengthening was observed between the bonds B_8-F_{10}, C_2-C_6, C_4-C_6, C_{23}-C_{25} by 0.02, 0.01, 0.01, 0.03 Å and bond lengths shortened for the bonds B_8-N_7, C_{25}-C_{29} by 0.01 and 0.03 Å respectively. Also boron atom, B_8, becomes displaced more by 0.09° and observed an increase in the bond angles, F_{10}-B_8-N_{11}, F_9-B_8-N_{11}, F_{10}-B_8-N_7 and F_9-B_8-N_7 by 0.96, 0.08, 0.93 and 0.14° respectively and decrease in the bond angle F_9-B_8-F_{10} by 2.48° in the diprotonated form (**1-2H EE**) compared to the neutral form (**1 EE**). A similar changes were observed for the dye **1 EZ** and its corresponding protonated form **1-2H EZ**.

In the excited state geometry the major bond lengthening was observed between the bonds B_8-F_{10}, C_2-C_6, C_4-C_6 and C_{23}-C_{25} by 0.01 Å each and the bond length shortening was observed only in C_{25}-C_{29} bond by 0.01 Å for molecule **1 EE,** whereas in case of its corresponding di protonated form, **1-2H EE**, bond lengthening was observed only in C_{25}-C_{29} bond by 0.01 Å whereas bond shortening was observed in C_{23}-C_{25} double bond by 0.01 Å.

The resulting ground state optimized geometry of the dyes **2 EE** and **2-2H EE** is such that it has a small dihedral angle C_{56}-C_1-C_{23}-C_{25} with one of the styryl subunit is off the C_9BF_2 plane as 15.29 and 4.92° and the other styryl subunit has dihedral angle C_{80}-C_{55}-C_{78}-C_{27} with C_9BF_2 plane as 15.3 and 4.93° respectively (Table 2). The excited state optimized geometry reveals that the styryl subunits become more planer compare to ground state in the dye **2 EE** with a decrease in the dihedral angle (C_{56}-C_1-C_{23}-C_{25} and C_{80}-C_{55}-C_{78}-C_{27}) by 6.2 and 5.68° respectively. Contrary to this was the observation with the corresponding diprotonated form **2-2H EE** in which there is an increase in dihedral angles (C_{56}-C_1-C_{23}-C_{25} and C_{80}-C_{55}-C_{78}-C_{27}) making the two styryl subunits more displaced from C_9BF_2 median plane by 1.85 and 1.84° respectively in excited state compare to ground state.

Upon protonation of the molecule **2 EE** to **2-2H EE**, the ground state optimized geometry reveals that a major

Table 1 Selected Bond lengths, Bond angles and Torsional angles of **1 EE** and **1 EZ**, and their corresponding diprotonated forms, using B3LYP 6-31G(d), (bond lengths are in Å, dihedral angles are in degree °)

Atom number	1 EE			1-2H EE		1 EZ			1-2H EZ	
	GAS	$CHCl_3$		$CHCl_3$		GAS	$CHCl_3$		$CHCl_3$	
	GS[a]	GS	ES[b]	GS[a]	ES[b]	GS[a]	GS	ES[b]	GS[a]	ES[b]
Bond lengths										
B_8-N_7	1.561	1.553	1.546	1.536	1.546	1.559	1.553	1.545	1.537	1.541
B_8-F_{10}	1.401	1.404	1.411	1.417	1.411	1.392	1.398	1.405	1.415	1.411
C_2-C_6	1.406	1.406	1.416	1.415	1.418	1.412	1.403	1.413	1.415	1.424
C_4-C_6	1.406	1.406	1.416	1.416	1.416	1.413	1.407	1.419	1.415	1.409
B_8-C_6	2.996	2.991	2.992	2.986	2.986	3.004	3.004	3.005	2.997	2.997
C_{23}–C_{25}	1.357	1.360	1.375	1.392	1.384	1.358	1.360	1.374	1.391	1.381
C_{25}–C_{29}	1.453	1.450	1.438	1.422	1.429	1.452	1.450	1.438	1.422	1.432
Bond angles										
C_2-N_7-B_8	124.2	124.0	124.2	124.1	124.1	125.5	125.2	125.4	125.3	125.4
F_9-B_8-F_{10}	110.3	109.5	108.7	107.0	107.6	110.1	109.5	108.6	107.1	107.6
F_{10}-B_8-N_{11}	109.9	110.1	110.2	111.1	110.7	110.3	110.4	110.5	110.9	110.8
F_9-B_8-N_{11}	110.2	110.2	110.6	110.3	110.1	110.5	110.5	110.7	110.8	110.6
F_{10}-B_8-N_7	109.9	110.1	110.2	111.1	110.7	109.9	109.9	110.0	110.8	110.5
F_9-B_8-N_7	110.2	110.1	110.6	110.3	110.2	108.8	108.9	109.3	109.1	108.8
Dihedral angles										
C_{56}-C_1-C_{23}-C_{25}	5.88	5.4	4.4	5.5	6.4	8.1	6.6	5.1	4.7	5.4
C_{80}-C_{55}-C_{78}-C_{27}	5.99	5.5	4.4	4.9	5.7	16.4	16.2	11.5	2.2	3.0
C_{14}-C_{12}-C_6-C_2	89.8	89.7	89.6	85.5	84.0	83.8	84.5	77.7	83.1	80.2
C_{13}-C_{12}-C_6-C_4	90.4	90.3	90.4	84.9	83.6	85.0	85.4	78.9	83.4	81.1

[a] Computed geometrical parameters of molecules in ground state

[b] Computed geometrical parameters of molecules in excited state

bond lengthening was observed between the bonds B_8-F_{10}, C_2-C_6, C_4-C_6, C_{23}-C_{25} by 0.015, 0.006, 0.006, 0.06 Å and the bond length shortening for the bonds B_8-N_7, C_{25}-C_{29} by 0.016 and 0.062 Å respectively and boron atom B_8 becomes displaced less by 0.62°. The observed increase in the bond angles, F_{10}-B_8-N_{11}, F_9-B_8-N_{11}, F_{10}-B_8-N_7 and F_9-B_8-N_7 was by 0.48, 0.69, 0.48 and 0.69° respectively and the decrease in bond angle F_9-B_8-F_{10} was by 2.22° in the di-protonated form, **2-2H EE**, compared to its neutral form, **2 EE**. A similar behavior was observed for the dye **2 EZ** and its corresponding protonated form **2-2H EZ**.

In the excited state geometry the major bond lengthening was observed between the bonds B_8-F_{10}, C_2-C_6, C_4-C_6 and C_{23}-C_{25} by 0.006, 0.01, 0.01, and 0.028 Å respectively and the bond length shortening observed only in C_{25}-C_{29} bond by 0.018 Å for molecule **2 EE**, where as in case of its corresponding di protonated form, **2-2H EE**, the bond lengthening between the bonds B_8-N_7, C_2-C_6, C_4-C_6 and C_{25}-C_{29} by 0.004, 0.002, 0.002, and 0.012 Å respectively and the bond length shortening observed in C_{23}-C_{25} and B_8-F_{10} bonds by 0.011 and 0.003 Å respectively.

Photophysical Properties of Dyes

Calculated Absorption Properties Of Dyes in Chloroform Media Before and After Protonation Using B3LYP/6-31G(d)

The calculated absorption spectra using TD-DFT have been compared with the observed results (Table 3) and it has been observed that for all studied molecules except di-protonated forms of **2 EE** and **2 EZ**, the absorption spectra calculated with B3LYP/6-31G(d) method in chloroform medium matches well with the experimental values [31].

Molecule **1 EE** show only deviation of 1.26 % (~8 nm) from the experimental value and shows major band with 100 % orbital contribution at 1.79 eV which is associated with H→L transition with oscillator strength of 1.104, but surprisingly its rotational isomer show even less deviation, that is 0.81 % (~6 nm) shows major band with 100 % orbital

Table 2 Selected Bond lengths, Bond angles and Torsional angles of **2 EE** and **2 EZ**, and their corresponding diprotonated forms using B3LYP 6-31G (d), (bond lengths are in Å, dihedral angles are in degree °)

Atom number	2 EE			2-2H EE		2 EZ			2-2H EZ	
	GAS	$CHCl_3$		$CHCl_3$		GAS	$CHCl_3$		$CHCl_3$	
	GS[a]	GS	ES[b]	GS[a]	ES[b]	GS[a]	GS	ES[b]	GS[a]	ES[b]
Bond lengths										
B_8-N_7	1.565	1.560	1.553	1.544	1.548	1.563	1.558	1.552	1.554	1.548
C_2–C_6	1.407	1.407	1.417	1.413	1.415	1.406	1.406	1.415	1.414	1.428
C_4–C_6	1.407	1.407	1.417	1.413	1.415	1.407	1.407	1.416	1.411	1.404
B_8-C_6	3.007	3.005	3.011	2.991	2.991	3.008	3.006	3.013	3.00	3.004
B_8-F_{10}	1.398	1.402	1.405	1.417	1.414	1.381	1.393	1.406	1.409	1.406
C_{23}–C_{25}	1.354	1.345	1.373	1.402	1.391	1.353	1.353	1.372	1.401	1.385
C_{29}–C_{25}	1.463	1.463	1.445	1.401	1.413	1.462	1.462	1.446	1.402	1.418
Bond angles										
C_2-C_7-B_8	124.7	124.8	124.7	1.544	1.548	125.6	125.5	125.4	124.9	125.1
F_9-B_8-F_{10}	110.8	110.2	109.5	1.413	1.415	109.9	110.4	109.1	108.2	108.6
F_{10}-B_8-N_{11}	109.5	109.6	109.8	1.413	1.415	109.6	110.2	110.1	110.2	110.1
F_9-B_8-N_{11}	110.3	110.3	110.6	2.991	2.991	110.3	110.3	110.5	110.9	110.9
F_{10}-B_8-N_7	109.5	109.6	109.8	1.417	1.414	108.3	108.1	108.7	110.2	110.1
F_9-B_8-N_7	110.6	110.3	110.6	1.402	1.391	110.3	110.2	110.4	109.7	109.0
Dihedral angles										
C_{56}-C_1-C_{23}-C_{25}	13.8	15.3	9.1	4.9	6.8	17.5	19.2	8.9	6.0	8.2
C_{59}-C_{55}-C_{57}-C_{27}	13.8	15.3	9.6	4.9	6.8	13.0	13.8	5.2	8.5	10.1
C_{14}-C_{12}-C_6-C_2	89.8	89.8	89.8	89.9	90.0	92.3	92.6	87.8	81.2	76.2
C_{13}-C_{12}-C_6-C_4	90.2	90.2	90.2	90.1	90.0	92.1	92.4	87.8	81.9	77.3

[a] Computed geometrical parameters of molecules in ground state

[b] Computed geometrical parameters of molecules in excited state

Table 3 Observed and computed photophysics of compounds in $CHCl_3$ using B3LYP/6-31G(d)

System	λ_{abs}[a] nm	TD-DFT								
		Absorption energy		%D[b]	f[c]	Major contribution	λ_{em}[d] (nm)	TD-DFT Emission (nm)	f	%D[b]
		nm	eV							
1 EE	700	691.2	1.79	1.26	1.104	H→L(100 %)	753	732.6	1.111	2.71
1 EZ	700	705.7	1.76	0.81	0.849	H→L(100 %)	753	750.3	0.861	0.36
1 2-H EE	615	611.8	2.02	0.52	0.294	H→L+1(72 %)	630	862.5	0.928	36.90
1 2-H EZ	615	605.5	2.04	1.54	0.281	H→L+1(67 %)	630	860.2	0.750	36.54
2 EE	620	592.1	2.09	4.50	0.943	H→L(100 %)	640	633.6	0.956	1.00
2 EZ	620	607.7	2.04	1.98	0.767	H→L(100 %)	640	649.2	0.754	1.44
2 2-H EE	670	800.6	1.54	19.49	0.800	H→L(95 %)	677	845.4	0.785	24.87
2 2-H EZ	670	801.5	1.54	19.63	0.693	H→L(95 %)	677	858.9	0.633	26.87

[a] Reported experimental absorption maximum wavelength

[b] Percent deviation from experimental absorption or emission maximum wavelength

[c] Oscillator strength

[d] Reported experimental emission maximum wavelength

contribution at 1.76 eV which is associated again with H→L transition with oscillator strength of 0.849. Similar are the observations for molecule **2 EE** that is band at 2.09 eV associated with H→L transition (4.50 % deviation with oscillator strength of 0.943) and its rotational isomer, **2 EZ**, band at 2.04 eV associated with H→L transition and 100 % orbital contribution (only 1.98 % deviation with oscillator strength of 0. 0.767). The less deviation in calculated absorption from experimental one for **1 EZ** and **2 EZ** compare to **1 EE** and **2 EE** supports the rotation about C_1-C_{23}/C_{55}-C_{78} bond.

Out of the two TD-DFT optimized di-protonated molecules, **1-2H EE** show vertical excitation at 611.8 nm associated with the H→L+1 with oscillator strength of 0.294 and 72 % orbital contribution, which is only deviated by 3.2 nm from the experimental value (615 nm), moreover its TD-DFT optimized rotational isomer, **1-2H EE**, also shows very good agreement between the calculated absorption spectra and experimental one with difference of only 9.5 nm (1.54 % deviation with oscillator strength of 0.281) which again support the possibility of rotation about C_1-C_{23}/C_{55}-C_{78} bond. On the other hand di-protonated forms of **2 EE** and **2 EZ** show more deviation of 19.49 % (130 nm). The TD-DFT optimized molecule **2-2H EE** and **2H EZ** both shows absorption maxima at 1.54 eV associated with the H→L electronic transition with oscillator strengths of 0.800 and 0.693 respectively. From the observed vertical excitation energies of the TD-DFT that is B3LYP/6-31G(d) optimized molecules, **1 EE**, **2 EE** and their corresponding rotational isomers, **1 EZ**, **2 EZ** in chloroform media, it can be concluded that molecules may be present in either of the forms as absorption maxima in case of **EZ** form is more closer with experimental one compare to **EE** form and there may be possibility of hydrogen bond formation between one of the fluorines and hydrogen which is present on next olefinic carbon, C_{25}/ C_{27} as it becomes closer to the one of the fluorines to form stronger hydrogen bonding.

Calculated Emission Properties of the Dyes in Chloroform Media Before and After Protonation using B3LYP/6-31G(d)

To obtain minimum energy geometries in excited state, the low-lying first singlet excited states (S1) of the dyes were relaxed using the TD-DFT and this excited state optimised geometry was used to obtain emission using TD-DFT and results are summarized in Table 3. From the obtained results it is revealed that there is good agreement between the experimental emissions [31] and emissions calculated using TD-DFT, B3LYP/6-31G(d) level of theory. The molecule **1 EE** and its corresponding rotamer, **1 EZ** show computed emission at 732.6 and 750.3 nm respectively while molecule **2 EE** and its corresponding rotamer, **2 EZ** show computed emission at 633.6 and 649.2 nm respectively however their experimental emissions are 753 and 640 nm. From this we can conclude that TD-DFT, B3LYP/6-31G(d) level of theory works very well for such kind of molecules as there is only 2.7 % deviation in emission of **1 EE**, 0.36 % in case of **1 EZ**, 1 and 1.44 % in case of **2 EE** and **2 EZ** respectively. From the emission results of di-protonated forms of **1 EE**, **2 EE, 1 EZ** and **2 EZ** it seems that TD-DFT, B3LYP/6-31G(d) level of theory cannot handle the calculations in excited state as deviations observed in computed emissions compare to experimental are ~36.5 % in case of **1-2H EE** and**1-2H EZ**. On the other hand **2-2H EE** and **2-2H EZ** show deviations of 25–27 %.

Dipole Moments

Computed Ground and Excited State Dipole Moments of the Compounds In Vacuum and $CHCl_3$ using B3LYP/6-31G(d)

The dipole moment of all the di-styryl BODIPYs, **1 EE**, **2 EE** and rotational isomers, **1 EZ**, **2 EZ**, and their corresponding di-protonated forms, **1 2-H EE, 2 2-H EE, 1 2-H EZ, 2 2-H EZ** in vacuum as well as chloroform medium calculated at B3LYP/6-31G(d) level of theory is summarized in Table 4. An increase in dipole moment was observed while going from gas phase to the solution phase (chloroform) viz for molecule **1 EE** and its rotamer, **1 EZ**, the increase in dipole moment in chloroform media was 1.84 D and 1.77 D respectively and for the molecule **2 EE** and its rotamer, **2 EZ**, the increase is 2.28 D and 2.3 D respectively. For molecules in its diprotonated forms, **1 2-H EE**, **2 2-H EE**, **1 2-H EZ**, **2 2-H EZ**, the effect becomes more prominent and the increase in dipole moment was observed to be 13.19 D, 13.36, 6.15 and 6.14 D respectively. This may be attributed to the presence of cationic charge in the molecule causing a large charge separation.

There was no much change observed in dipole moment on rotation of about C1-C23/C25-C78 single bond, the difference between the dipole moment of **1 EE** and its rotamer **1 EZ** is only 0.06 D in the ground state and 0.14 D in excited state respectively. Similar are the observations for corresponding di-protonated forms as well as for molecule **2 EE**, **2 EZ** and their corresponding di-protonated forms (Table 4).

The most important thing is when we compare the dipole moments of molecules with its di-protonated forms in vacuum as well as in chloroform media calculated at B3LYP/6-31G(d) level of theory shows that there is a considerable increase in dipole moment after di-protonation of **1 EE** and its rotamer **1 EZ** by 27.83 D and 27.71 D in vacuum and 39.17 D and 39.3 D in chloroform media respectively. A similar trend was observed for molecule **2 EE** and its rotamer, **2 EZ** upon di-protonation (Table 4).

Table 4 Computed ground and excited state dipole moments of the compounds in vacuum and $CHCl_3$ using B3LYP/6-31G(d)

Molecule	Vacuum	$CHCl_3$					$\mu_g{}^a{}_{(CHCl3)}$ $-\mu_g{}^a{}_{(GAS)}$
	$\mu_g{}^a$	$\mu_g{}^a$	$\mu_e{}^b$	$\mu_e{}^b$- $\mu_g{}^a$	$EE\mu_g{}^a$- $EZ\mu_g{}^a$	$EE\mu_e{}^b$- $EZ\mu_e{}^b$	
1 EE	03.80	05.65	06.63	0.98	0.06	0.14	01.84
1 EZ	03.82	05.59	06.49	0.90			01.77
1 2-H EE	31.63	44.82	45.16	0.34	−0.07	−0.59	13.19
1 2-H EZ	31.53	44.89	45.75	0.86			13.36
2 EE	09.41	11.69	11.81	0.12	0.24	0.29	02.28
2 EZ	09.15	11.45	11.52	0.07			02.30
2 2-H EE	11.98	18.13	18.98	0.85	0.09	−0.29	06.15
2 2-H EZ	11.90	18.04	19.27	1.23			06.14

[a] Dipole moment of compound in ground state

[b] Dipole moment of compound in excited state

Molecular Orbital Energies

Energy levels of the frontier molecular orbitals especially HOMO and LUMO as well as their spatial distributions are deciding parameters for photophysical properties. The density plot of the HOMO and LUMO of dyes, **1 EE**, **2EE**, their diprotonated forms and **1 EZ**, **2 EZ,** their diprotonated forms are calculated at B3LYP/6-311G(d) level of theory and are shown in Figs. 2 and 3 respectively

The orbital diagrams are plotted with the contour value of 0.02 a. u. The plots of the HOMO and LUMO of the studied molecules have the typical π molecular orbital characteristics and are not or slightly altered by the C-C single bond rotation about C_1-C_{23}/C_{55}-C_{78} bond. From the molecular orbital analysis, we conclude that the lowest lying singlet-singlet absorption as well as emission corresponds to π→π* type of the electronic transition. From the Figs. 2 and 3 it is revealed that, for

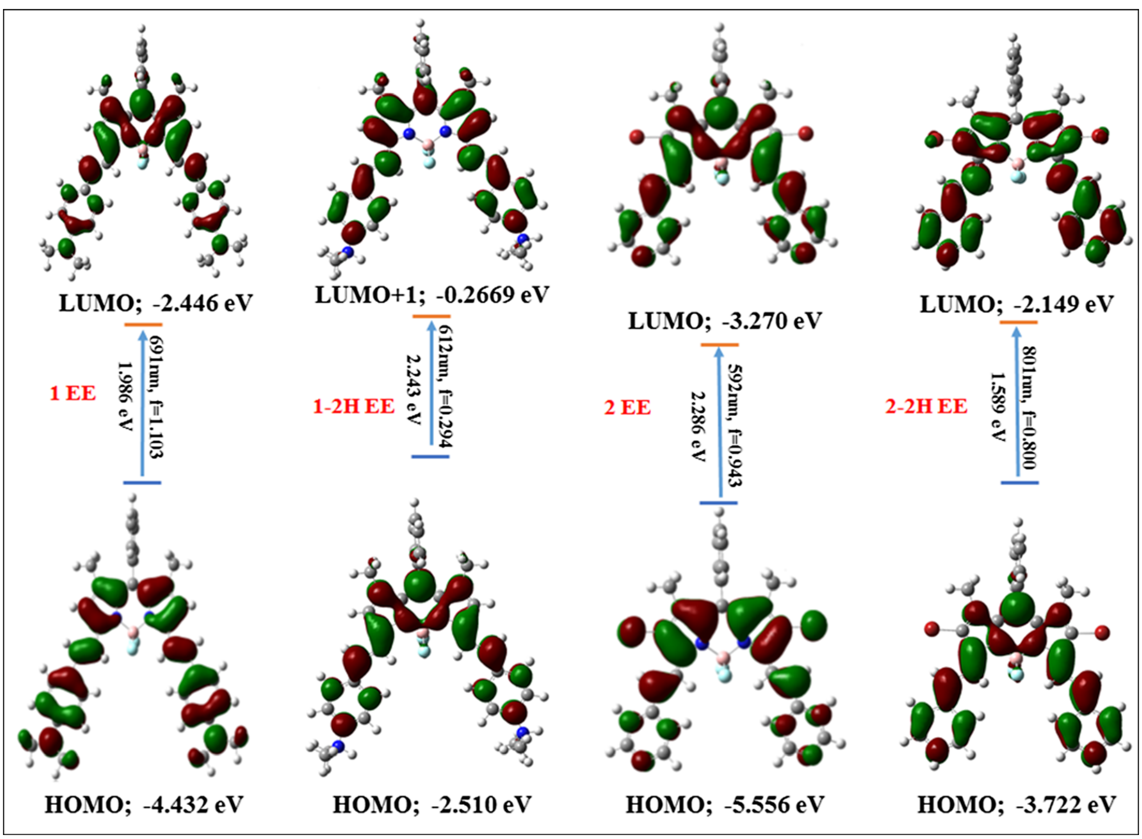

Fig. 2 Frontier molecular orbitals of compound **1 EE, 2 EE** and their corresponding di-protonated forms, **1-2H EE, 2-2H EE**, at ground state

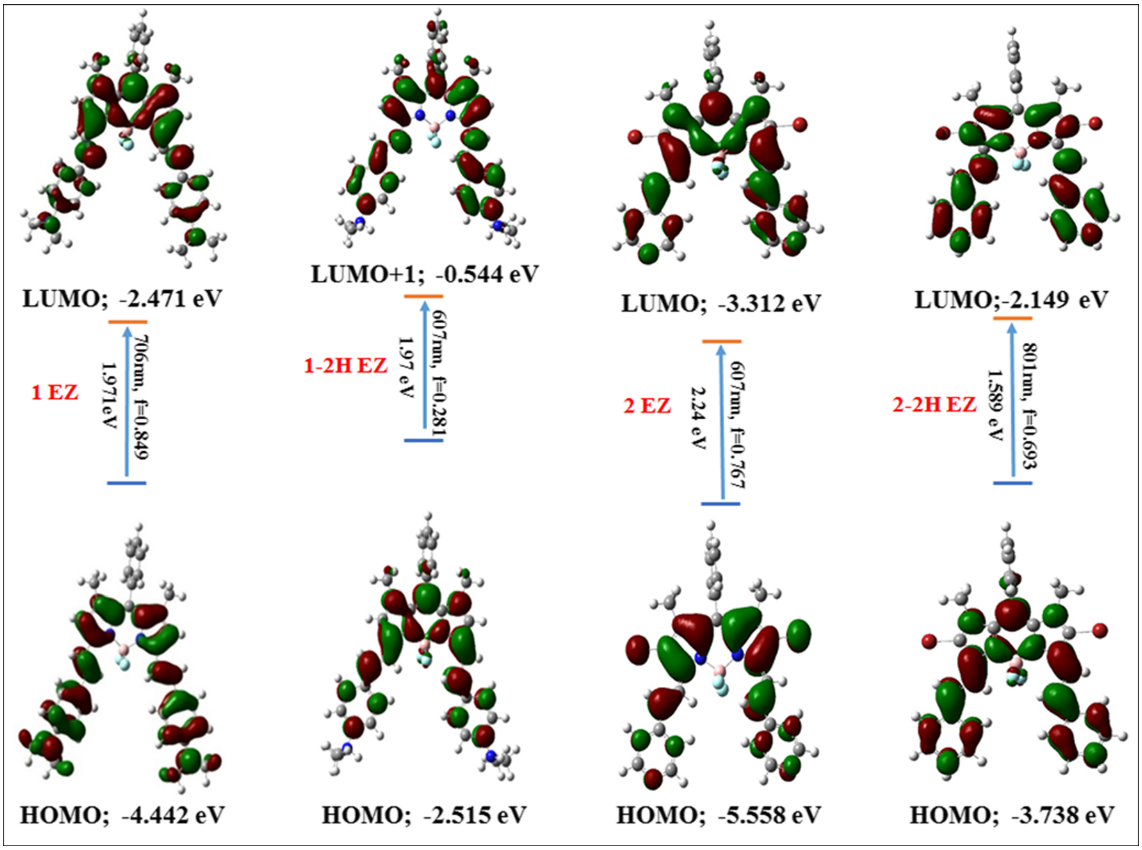

Fig. 3 Frontier molecular orbitals of compound **1 EZ, 2 EZ** and their corresponding di-protonated forms, **1-2H EZ, 2-2H EZ**, at ground state

molecule **1 EE**, and its rotamer, **1 EZ,** HOMO are mainly delocalized over entire molecule except group at *meso* position and LUMO is delocalized mainly on BODIPY core, C_9BF_2 framework. For di-protonated forms, **1-2H EE** and **1-2H EZ**, as expected, reverse is observed that is HUMO is delocalized mainly on BODIPY core and LUMO+1 is delocalized mainly on styryl subunits clearly indicates after protonation in presence of trifluoroacetic acid, N, N-dimethyl aniline becomes electron withdrawing moiety which withdraws electrons from the main chromophore, BODIPY core, making it electron deficient causing absorption as well as emission becomes blue shifted.

For molecules **2 EE** and **2 EZ**, HOMO are delocalized mainly over C_9BF_2 framework but LUMO is delocalized over entire system except orthogonal *meso* group which supports the electron withdrawing nature of the pyridine nitrogen at 4-position through extended conjugation and this is because **2 EE**/**2 EZ** is blue shifted compare to **1 EE**/**2 EZ**. Whereas for di-protonated forms, **2-2H EE** and **2-2H EZ** HUMO is delocalized mainly on styryl subunits as pyridyl nitrogen at 4 position withdraws electron effectively and LUMO is delocalized predominantly again on styryl subunits.

Conclusions

To this end we can conclude that, we have studied properties like structural geometries of di-styryl BODIPY molecules at ground and excited state using DFT at B3LYP/6-31G(d) level of theory. Computed absorption and emission spectra of **1 EE**, **2 EE** and their rotamers, **1 EZ**, **2 EZ**, were in very good agreement with the experimental values. Also calculated absorption spectra of diprotonated forms, **1-2H EE** and **1-2H EZ** of **1 EE** and its rotamer, **1 EZ**, respectively shows negligible deviation from experimental spectra. From the calculated absorption spectra of **2-2H EE** and **2-2H EZ** and emission spectra of **1-2H EE**, **1-2H EZ, 1-2H EE**, and **1-2H EZ** it can be concluded that the B3LYP/6-31G(d) level of theory cannot handle calculations of this molecule as deviations from experimental values are greater and can be attempted using theory with a different function(s) and or higher basis set(s).

Acknowledgments One of the authors, Kishor G. Thorat, is very thankful to CSIR for financial assistance.

References

1. Treibs A, Kreuzer F-H (1968) Difluorboryl-Komplexe von Di- und Tripyrrylmethenen. Justus Liebigs Ann der Chem 718:208–223. doi:10.1002/jlac.19687180119
2. Haugland RP (2005) the handbook: a guide to fluorescent probes and labeling technologies, 10th ed. 1126
3. Coskun A, Akkaya EU (2005) Ion sensing coupled to resonance energy transfer: a highly selective and sensitive ratiometric fluorescent chemosensor for Ag(I) by a modular approach. J Am Chem Soc 127:10464–10465. doi:10.1021/ja052574f
4. Rurack K, Kollmannsberger M, Resch-Genger U, Daub J (2000) A selective and sensitive fluoroionophore for Hg II, Ag I, and Cu II with virtually decoupled fluorophore and receptor units. J Am Chem Soc 122:968–969. doi:10.1021/ja992630a
5. Coskun A, Akkaya EU (2006) Signal ratio amplification via modulation of resonance energy transfer: proof of principle in an emission ratiometric Hg(II) sensor. J Am Chem Soc 128:14474–14475. doi:10.1021/ja066144g
6. Zeng L, Miller EW, Pralle A et al (2006) A selective turn-on fluorescent sensor for imaging copper in living cells. J Am Chem Soc 128:10–11. doi:10.1021/ja055064u
7. Coskun A, Deniz E, Akkaya EU (2005) Effective PET and ICT switching of boradiazaindacene emission: a unimolecular, emission-mode, molecular half-subtractor with reconfigurable logic gates. Org Lett 7:5187–5189. doi:10.1021/ol052020h
8. Saki N, Dinc T, Akkaya EU (2006) Excimer emission and energy transfer in cofacial boradiazaindacene (BODIPY) dimers built on a xanthene scaffold. Tetrahedron 62:2721–2725. doi:10.1016/j.tet.2005.12.021
9. Coskun A, Baytekin BT, Akkaya EU (2003) Novel fluorescent chemosensor for anions via modulation of oxidative PET: a remarkable 25-fold enhancement of emission. Tetrahedron Lett 44:5649–5651. doi:10.1016/S0040-4039(03)01365-0
10. Ekmekci Z, Yilmaz MD, Akkaya EU (2008) A monostyryl-boradiazaindacene (BODIPY) derivative as colorimetric and fluorescent probe for cyanide ions. Org Lett 10:461–464. doi:10.1021/ol702823u
11. Li F, Yang SI, Ciringh Y et al (1998) Design, synthesis, and photodynamics of light-harvesting arrays comprised of a porphyrin and one, two, or eight boron-dipyrrin accessory pigments. J Am Chem Soc 120:10001–10017. doi:10.1021/ja9812047
12. Yilmaz MD, Bozdemir OA, Akkaya EU (2006) Light harvesting and efficient energy transfer in a boron-dipyrrin (BODIPY) functionalized perylenediimide derivative. Org Lett 8:2871–2873. doi:10.1021/ol061110z
13. Loudet A, Burgess K (2007) BODIPY dyes and their derivatives: syntheses and spectroscopic properties. Chem Rev 107:4891–4932. doi:10.1021/cr078381n
14. Wood TE, Thompson A (2007) Advances in the chemistry of dipyrrins and their complexes. Chem Rev 107:1831–1861. doi:10.1021/cr050052c
15. Ziessel R, Ulrich G, Harriman A (2007) The chemistry of Bodipy: a new El Dorado for fluorescence tools. New J Chem 31:496. doi:10.1039/b617972j
16. Weissleder R (2001) A clearer vision for in vivo imaging. Nat Biotechnol 19:316–317. doi:10.1038/86684
17. Burghart A, Kim H, Welch MB et al (1999) 3,5-Diaryl-4,4-difluoro-4-bora-3a,4a-diaza-s-indacene (BODIPY) Dyes: synthesis, spectroscopic, electrochemical, and structural properties. J Org Chem 64:7813–7819. doi:10.1021/jo990796o
18. Yamada K, Toyota T, Takakura K et al (2001) Preparation of BODIPY probes for multicolor fluorescence imaging studies of membrane dynamics. New J Chem 25:667–669. doi:10.1039/b100757m
19. Killoran J, Allen L, Gallagher JF, et al. (2002) Synthesis of BF2 chelates of tetraarylazadipyrromethenes and evidence for their photodynamic therapeutic behaviour. Chemical Communications 1862–1863. doi: 10.1039/b204317c
20. Gorman A, Killoran J, O'Shea C et al (2004) In vitro demonstration of the heavy-atom effect for photodynamic therapy. J Am Chem Soc 126:10619–10631. doi:10.1021/ja047649e
21. Chen J, Burghart A, Derecskei-Kovacs A, Burgess K (2000) 4,4-Difluoro-4-bora-3a,4a-diaza- s -indacene (BODIPY) dyes modified for extended conjugation and restricted bond rotations. J Org Chem 65:2900–2906. doi:10.1021/jo991927o
22. Zhao W, Carreira EM (2005) Conformationally restricted aza-bodipy: a highly fluorescent, stable, near-infrared-absorbing dye. Angew Chem (Int ed Engl) 44:1677–1679. doi:10.1002/anie.200461868
23. Zhao W, Carreira EM (2006) Conformationally restricted aza-BODIPY: highly fluorescent, stable near-infrared absorbing dyes. Chem (Weinheim Bergstrasse, Germany) 12:7254–7263. doi:10.1002/chem.200600527
24. Chen J, Burghart A, Wan C-W et al (2000) Synthesis and spectroscopic properties of 2-ketopyrrole–BF2 complexes: a new class of fluorescent dye. Tetrahedron Lett 41:2303–2307. doi:10.1016/S0040-4039(00)00166-0
25. Wada M, Ito S, Uno H et al (2001) Synthesis and optical properties of a new class of pyrromethene–BF2 complexes fused with rigid bicyclo rings and benzo derivatives. Tetrahedron Lett 42:6711–6713. doi:10.1016/S0040-4039(01)01299-0
26. Shen Z, Röhr H, Rurack K et al (2004) Boron-diindomethene (BDI) dyes and their tetrahydrobicyclo precursors–en route to a new class of highly emissive fluorophores for the red spectral range. Chem (Weinheim Bergstrasse, Germany) 10:4853–4871. doi:10.1002/chem.200400173
27. Goeb S, Ziessel R (2007) Convenient synthesis of green diisoindolodithienylpyrromethene-dialkynyl borane dyes. Org Lett 9:737–740. doi:10.1021/ol0627404
28. Umezawa K, Nakamura Y, Makino H et al (2008) Bright, color-tunable fluorescent dyes in the visible-near-infrared region. J Am Chem Soc 130:1550–1551. doi:10.1021/ja077756j
29. Rurack K, Kollmannsberger M, Daub J (2001) Molecular switching in the near infrared (NIR) with a functionalized boron-dipyrromethene dye this work was supported by the Deutsche Forschungsgemeinschaft (Da 92/24-1). Angew Chem (Int ed Engl) 40:385–387. doi:10.1002/1521-3773
30. Atilgan S, Ekmekci Z, Dogan AL, et al. (2006) Water soluble distyryl-boradiazaindacenes as efficient photosensitizers for photodynamic therapy. Chemical communications (Cambridge, England) 4398–400. doi:10.1039/b612347c
31. Deniz E, Isbasar GC, Bozdemir OA et al (2008) Bidirectional switching of near IR emitting boradiazaindacene fluorophores. Org Lett 10:3401–3403. doi:10.1021/ol801062h
32. Atilgan S, Ozdemir T, Akkaya EU (2008) A sensitive and selective ratiometric near IR fluorescent probe for zinc ions based on the distyryl-bodipy fluorophore. Org Lett 10:4065–4067. doi:10.1021/ol801554t
33. Atilgan S, Kutuk I, Ozdemir T (2010) A near IR di-styryl BODIPY-based ratiometric fluorescent chemosensor for Hg(II). Tetrahedron Lett 51:892–894. doi:10.1016/j.tetlet.2009.12.025
34. Zhang X, Xiao Y, Qi J et al (2013) Long-wavelength, photostable, two-photon excitable BODIPY fluorophores readily modifiable for molecular probes. J Org Chem 78:9153–9160. doi:10.1021/jo401379g

35. Zhao C, Zhang Y, Wang X, Cao J (2013) Development of BODIPY-based fluorescent DNA intercalating probes. J Photochem Photobiol A Chem 264:41–47
36. Zheng Q, Xu G, Prasad PN (2008) Conformationally restricted dipyrromethene boron difluoride (BODIPY) dyes: highly fluorescent, multicolored probes for cellular imaging. Chem (Weinheim Bergstrasse, Germany) 14:5812–5819. doi:10.1002/chem.200800309
37. Puntoriero F, Nastasi F, Bura T et al (2011) Molecular logics: a mixed bodipy–bipyridine dye behaving as a concealable molecular switch. New J Chem 35:948. doi:10.1039/c0nj00770f
38. Kolemen S, Bozdemir OA, Cakmak Y et al (2011) Optimization of distyryl-Bodipy chromophores for efficient panchromatic sensitization in dye sensitized solar cells. Chem Sci 2:949. doi:10.1039/c0sc00649a
39. Kolemen S, Cakmak Y, Erten-Ela S et al (2010) Solid-state dye-sensitized solar cells using red and near-IR absorbing Bodipy sensitizers. Org Lett 12:3812–3815. doi:10.1021/ol1014762
40. Erten-Ela S, Yilmaz MD, Icli B et al (2008) A panchromatic boradiazaindacene (BODIPY) sensitizer for dye-sensitized solar cells. Org Lett 10:3299–3302. doi:10.1021/ol8010612
41. Zhao Y, Zhang Y, Lv X et al (2011) Through-bond energy transfer cassettes based on coumarin–Bodipy/distyryl Bodipy dyads with efficient energy efficiences and large pseudo-Stokes' shifts. J Mater Chem 21:13168. doi:10.1039/c1jm12503f
42. Guliyev R, Coskun A, Akkaya EU (2009) Design strategies for ratiometric chemosensors: modulation of excitation energy transfer at the energy donor site. J Am Chem Soc 131:9007–9013. doi:10.1021/ja902584a
43. Eggenspiller A, Takai A, El-Khouly ME et al (2012) Synthesis and photodynamics of fluorescent blue BODIPY-porphyrin tweezers linked by triazole rings. J Phys Chem A 116:3889–3898. doi:10.1021/jp300415a
44. Qin W, Baruah M, De Borggraeve WM, Boens N (2006) Photophysical properties of an on/off fluorescent pH indicator excitable with visible light based on a borondipyrromethene-linked phenol. J Photochem Photobiol A Chem 183:190–197. doi:10.1016/j.jphotochem.2006.03.015
45. Rurack K, Kollmannsberger M, Daub J (2001) Molekulares Schalten im nahen Infrarot (NIR) mit einem funktionalisierten Bordipyrromethen-Farbstoff. Angew Chem 113:396–399. doi:10.1002/1521-3757(20010119)113:2<396::AID-ANGE396>3.0.CO;2-W
46. Frisch MJ, Trucks GW, Schlegel HB, et al. (2009) Gaussian 09 C.01
47. Treutler O, Ahlrichs R (1995) Efficient molecular numerical integration schemes. J Chem Phys 102:346. doi:10.1063/1.469408
48. Becke AD (1993) A new mixing of Hartree–Fock and local density-functional theories. J Chem Phys 98:1372. doi:10.1063/1.464304
49. Lee C, Yang W, Parr RG (1988) Development of the Colle-Salvetti correlation-energy formula into a functional of the electron density. Phys Rev B 37:785–789. doi:10.1103/PhysRevB.37.785
50. Hehre WJ (1976) Ab initio molecular orbital theory. Acc Chem Res 9:399–406. doi:10.1021/ar50107a003
51. Bauernschmitt R, Ahlrichs R (1996) Treatment of electronic excitations within the adiabatic approximation of time dependent density functional theory. Chem Phys Lett 256:454–464. doi:10.1016/0009-2614(96)00440-X
52. Furche F, Rappoport D (2005) Computational photochemistry (Google eBook). 368
53. Gabe Y, Ueno T, Urano Y et al (2006) Tunable design strategy for fluorescence probes based on 4-substituted BODIPY chromophore: improvement of highly sensitive fluorescence probe for nitric oxide. Anal Bioanal Chem 386:621–626. doi:10.1007/s00216-006-0587-y
54. Furche F, Ahlrichs R (2002) Adiabatic time-dependent density functional methods for excited state properties. J Chem Phys 117:7433. doi:10.1063/1.1508368
55. Leszczynski J, Shukla M (2009) Practical aspects of computational chemistry: methods. Concepts Appl (Google eBook) 484
56. Scalmani G, Frisch MJ, Mennucci B et al (2006) Geometries and properties of excited states in the gas phase and in solution: theory and application of a time-dependent density functional theory polarizable continuum model. J Chem Phys 124:94107. doi:10.1063/1.2173258
57. Valeur B, Berberan-Santos MN (2013) Molecular fluorescence: principles and applications (Google eBook), 2 nd. 500
58. Cossi M, Barone V, Cammi R, Tomasi J (1996) Ab initio study of solvated molecules: a new implementation of the polarizable continuum model. Chem Phys Lett 255:327–335. doi:10.1016/0009-2614(96)00349-1
59. Tomasi J, Mennucci B, Cammi R (2005) Quantum mechanical continuum solvation models. Chem Rev 105:2999–3093. doi:10.1021/cr9904009